Research Horizon

ISSN: 2808-0696 (p), 2807-9531 (e)

Research Horizon
Volume: 06
Issue: 05
Year: 2026
Page: 2385-2396

Citation:
Ridlo, D. T., Kurniawan, A., Fadli, Pranajati, A., Firmansyah, M. T., & Kautsar, R. A. (2026). Peak power analysis of an off-grid solar PV system during AC pump startup. *Research Horizon*, *6*(5), 2385-2396.

Article History:
Received: September 13, 2026
Revised: October 14, 2026
Accepted: October 18, 2026
Online since: October 25, 2026

Peak Power Analysis of an Off-Grid Solar PV System During AC Pump Startup

Dimas Taufiq Ridlo[1*], Adi Kurniawan[1], Fadli[1], Andi Pranajati[2], Muhammad Taufiq Firmansyah[1], Rehydra Al Kautsar[1]

[1] Department of Energy Systems Engineering, Faculty of Industrial Technology and Energy, Institut Teknologi Yogyakarta, Yogyakarta, Indonesia
[2] Department of Mining Engineering, Institut Teknologi Yogyakarta, Yogyakarta, Indonesia

[*] *Corresponding author: Dimas Taufiq Ridlo (dimas.taufiq.r@ity.ac.id)*

Abstract

Off-grid photovoltaic water pumping systems must accommodate changes in electrical demand during AC pump startup, which steady-state power alone may not represent. This study characterizes an AC pump's startup power profile in an off-grid solar photovoltaic system and examines its relevance to inverter selection. A prototype comprising a 585 Wp PV panel, a 12 V, 100 Ah LiFePO4 battery, a 2,000 W inverter, and an AC pump was evaluated. A camera recorded the power-measuring instrument's display, and values were transcribed across pre-startup, transient, and steady-state phases. Ten tests were analyzed using peak power, steady-state power, time to peak, transient duration, and the peak-to-steady-state power ratio. Peak startup power ranged from 125 to 200 W, averaging 157.0 W, whereas steady-state power ranged from 88 to 92 W, averaging 90.0 W. The mean ratio was 1.74, and the transient lasted 2.8–3.8 s. Startup demand exceeded steady-state demand and varied more across tests. Inverter assessment should consider startup behavior alongside continuous power requirements. Because measurements relied on a display, observed peaks do not represent sub-cycle electrical peaks.

Keywords

AC Pump, Inverter Capacity, Off-Grid Photovoltaic System, Peak Startup Power, Transient Power, Water Pumping.

1. Introduction

Photovoltaic Water Pumping (PVWP) systems are gaining attention as a solution for water supply for irrigation and community needs in remote areas not yet connected to the electrical grid. These systems integrate Photovoltaic (PV) modules, power conditioners, energy storage or buffering devices, inverters or motor drivers, electric motors, and water pumps. Their operational effectiveness is determined by the proper sizing of each component, the characteristics of the motor-pump unit, solar irradiation levels, and the specific operational strategies employed (Gevorkov et al., 2022; Belgacem et al., 2022; Suratno & Cahyono, 2023). Designing a PVWP system requires an integrated approach to ensure that the generated energy is optimally converted into mechanical power to meet water-pumping requirements. In off-grid PVWP systems, power-supply reliability is critical because the electrical grid provides no direct support during power drops or transient disturbances.

Consequently, sufficient power capacity and operational stability become the primary determinants of system success (Suwito et al., 2022; Zhou et al., 2024; Yogaswara & Korry, 2025). Furthermore, pump load characteristics are dynamic and change throughout the startup, acceleration, and steady-state operational phases. Evaluating system performance cannot rely solely on power measurements taken during normal operation; it must also account for initial power requirements, load fluctuations, and the system's ability to maintain operation under varying solar irradiation conditions (Wanyama et al., 2023). This approach is essential for establishing an adequate power margin and improving the efficiency and reliability of solar-powered pumping systems.

PVWP generally focuses on the optimization of Maximum Power Point Tracking (MPPT), motor control, system sizing, energy efficiency, and the enhancement of hydraulic performance to optimize the water-pumping process (Bawa et al., 2025). However, beyond performance under normal operating conditions, the motor-starting process also warrants attention because it can lead to high inrush currents, voltage sags, and transient power demands. Such conditions may compromise system stability, particularly when the energy source has limited capacity or the system operates in an "islanded" mode, independent of the main power grid (Ismail et al., 2024; Saady et al., 2025).

Several studies have addressed the impact of motor starting on power supply stability. Hermawan et al. (2023) demonstrated the use of photovoltaic energy sources to help mitigate voltage sags caused by inrush currents in induction motors, while Habyarimana et al. (2022) emphasized that the current during the acceleration (run-up) phase of a large-capacity induction motor can significantly exceed its nominal current. Nevertheless, a high initial current ratio does not necessarily translate into a proportional increase in active power, as the relationship between the two is influenced by the power factor, inverter dynamics, and the measurement characteristics of the instrumentation.

Evaluating power requirements during startup, separately from power measurements taken under steady-state conditions, provides a more accurate picture of a PVWP system's ability to meet transient power demands and maintain operational reliability. This study focuses on a simple, direct measurement of the system's output power profile during AC pump startup. Unlike research that optimizes MPPT algorithms or motor controllers, this study contributes by deriving key parameters, namely peak power, time-to-peak, transient duration, steady-state power, and the ratio of peak power to steady-state power, through field measurements captured via video recordings of the measuring instruments' displays. The objective is to quantify the instantaneous power surge during AC pump startup and evaluate its implications for inverter surge-capacity requirements in off-grid

solar photovoltaic systems. The findings are intended to provide a practical basis for avoiding inverter selection based solely on a pump's steady-state operating power.

2. Literature Review

2.1. Photovoltaic Water Pumping Systems

Photovoltaic Water Pumping (PVWP) systems use solar energy to supply electrical power for water pumping, particularly in locations with limited access to the electrical grid. A typical PVWP system consists of PV modules, power conditioning equipment, an inverter or motor drive, an electric motor, and a water pump. PV modules convert solar irradiance into electrical energy, which is subsequently supplied to the motor-pump unit according to the system configuration. Periasamy et al. (2015) reviewed the development and configurations of PVWP systems, highlighting their application for water supply. In directly coupled configurations, system performance depends on the compatibility between the PV array and the motor-pump unit, as well as the available solar energy (Kolhe et al., 2004). These characteristics make component selection and system integration important for reliable pumping operation.

In PVWP systems using AC pumps, the inverter or motor drive converts available electrical power into a supply suitable for operating the motor. Converter design and energy conversion efficiency are therefore important considerations in autonomous PVWP applications (Caracas et al., 2013). System performance is also influenced by variations in solar irradiance, conversion losses, and electrical component compatibility. Benlarbi et al. (2004) investigated global efficiency optimization in a PVWP system, demonstrating the relevance of efficiency considerations in system operation. Furthermore, motor-drive configuration affects how electrical power is delivered to the pump; for example, Singh et al. (2018) examined a standalone PV water-pumping system using an induction motor drive with reduced sensors. During startup, the motor's power requirements may differ substantially from those under steady-state conditions because the motor must accelerate before reaching normal operation. Therefore, both steady-state power consumption and transient power requirements should be considered when assessing inverter suitability for PVWP systems.

2.2. Motor Startup Characteristics and Transient Power Requirements

The startup of an Alternating-Current (AC) motor is characterized by transient electrical conditions that differ from those during steady-state operation. At startup, an induction motor can draw a high inrush current because the rotor has not yet reached its operating speed. This current gradually decreases as the motor accelerates toward steady-state, although the magnitude and duration of the transient depend on the motor characteristics and starting conditions. Habyarimana et al. (2022) explained that high starting and acceleration currents can cause voltage drops and place additional demands on power supply systems with limited capacity. In standalone PV applications, these effects are particularly important because the available power is constrained by solar generation and the capacity of the electrical components. Bahramian et al. (2025) further demonstrated that motor startup can cause PV voltage drops and converter instability in battery-less off-grid systems. Therefore, when assessing the electrical requirements of PV-powered pumping systems, startup performance must be distinguished from steady-state operation.

Evaluating transient power requirements involves identifying the peak power, time to peak power, transient duration, steady-state power, and ratio of peak power to steady-state power. These parameters characterize the magnitude and duration of the startup power surge relative to normal operation. Singh and Shukla (2018) investigated the starting and steady-state performance of an induction motor drive for PV water pumping, illustrating the relevance of evaluating both operating

conditions in PV-powered motor applications. For off-grid PVWP systems, the observed peak power provides an important reference for assessing inverter surge capacity, while steady-state power indicates the demand during normal operation (Angadi et al., 2021). Selecting an inverter based solely on the pump's steady-state power may therefore overlook the additional demand during startup. Assessing the startup power profile can provide a practical basis for determining whether the inverter can accommodate transient demands while maintaining reliable pump operation.

3. Methods

The research object is a prototype of an off-grid solar PV system designed to power an AC pump. The system comprises a 585 Wp solar panel, an MPPT solar charge controller, a 12 V, 100 Ah Lithium Iron Phosphate (LiFePO4) battery with a nominal energy capacity of 1.2 kWh, a 12 V-to-AC inverter rated at 2,000 W, and an AC booster/circulation pump. The pump's power consumption, estimated at approximately 120 W in the progress report, requires verification through actual measurement. The system is equipped with Miniature Circuit Breakers (MCBs) on the PV, battery, and output sides for electrical protection. Table 1 and Figure 1 show the prototype configuration.

Table 1. Test System Prototype

Component	Specifications/Conditions
Solar panel	One unit; 585 Wp; N-type monocrystalline half-cell
Solar charge controller	PowMr MPPT charge controller
Energy storage	LiFePO4 battery, 12 V, 100 Ah, nominal energy capacity of 1,200 Wh
Inverter	Taffware NB2000V; 12 V input; rated capacity of 2,000 W
AC pump	Shimizu PS-128 BIT non-automatic shallow-well pump, 220 V, 125 W output power, 290 W input power, maximum suction depth of 9 m, maximum total head of 33 m, maximum capacity of 33 L/min
Protection	PV-side, battery-side, and output-side MCBs
Data acquisition	Video recording of the power-measuring instrument's display

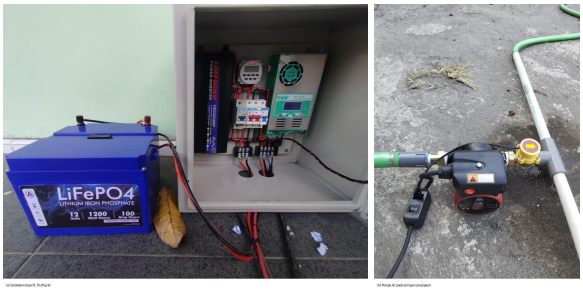


Figure 1. Prototype of the Off-Grid Solar PV System and AC Pump

Data acquisition is performed using a camera positioned at a fixed location and aimed at the power-measuring instrument display. The camera serves solely as a recording medium, allowing frame-by-frame review of the displayed power values. Recording begins before the pump is activated and continues until the power reaches steady state. The time origin (t=0) is defined as the moment the pump's ON command is issued. The recorded values are subsequently transcribed into a time-versus-power dataset covering the pre-startup, transient, and steady-state phases. To establish the measurement method's temporal resolution and limitations, the camera's frame rate, the measuring instrument's type and resolution or accuracy, the instrument's installation point, and the display update rate are documented. The

configuration of the off-grid solar PV system and the power-display recording arrangement during AC pump startup are illustrated in Figure 2.

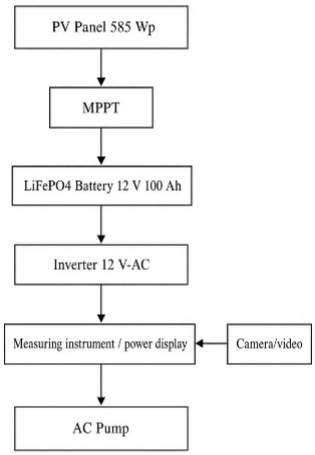


Figure 2. System Block Diagram and Power-Display Recording Method

The primary parameters analyzed include the pre-startup power (P_0), peak startup power (P_{peak}), time to peak power (t_{peak}), steady-state operating power (P_{ss}), transient duration (ttr), and peak-to-steady-state power ratio (K_p). The ratio K_p quantifies the magnitude of the observed peak startup power relative to the steady-state operating power and is calculated using Equation (1):

$$K_p = \frac{P_{\text{peak}}}{P_{\text{ss}}} \tag{1}$$

The percentage increase in peak power relative to steady-state power is calculated using Equation (2):

$$\Delta P(\%) = \frac{P_{\text{peak}} - P_{\text{ss}}}{P_{\text{ss}}} \times 100\% \tag{2}$$

The results are summarized as the minimum, maximum, mean, and standard deviation. Due to limited temporal resolution, peak power represents the highest recorded value rather than the instantaneous electrical peak within an AC cycle. Each trial begins with the system stabilized, and baseline power is recorded before pump activation. Power readings are then recorded throughout startup and steady-state operation. Video recordings are reviewed to determine P_{peak}, t_{peak}, P_{ss}, and ttr. Ten trials are conducted within the same testing period. Battery condition and voltage, weather, solar irradiance, intervals between successive starts, and ambient temperature are controlled where feasible or documented to account for trial-to-trial variation.

4. Results

Research results indicate that real-time power changes significantly during startup when equipment is first put into operation. In the initial phase, power demand tends to rise due to the inrush current (starting current) required to drive the equipment until it reaches normal operating conditions. Once startup is complete, power consumption gradually adjusts to load requirements and the system's operating state. Real-time power monitoring allows direct observation of energy-consumption fluctuations, which can be used to evaluate electrical-system

performance, identify power surges, and assess the equipment's efficiency and operational stability.

Table 2. Real-time Power Data

Time (s)	Power (W)	Condition
−3.0	13	System ON, pump OFF
−2.0	13	System ON, pump OFF
−1.0	13	System ON, pump OFF
0.0	13	Pump ON command
0.2	65	Initial start
0.4	125	Power increasing
0.6	200	Starting peak
0.8	184	Transient
1.0	165	Transient
1.5	138	Transient
2.0	115	Approaching stability
2.5	101	Approaching stability
3.0	94	Near-stable
3.5	91	Stable
4.0	90	Stable
5.0	91	Stable
6.0	90	Stable
8.0	90	Stable
10.0	91	Stable

When the system is powered on without activating the pump, the display indicates a baseline power of approximately 13 W, representing the initial system consumption. After the "ON" command, power gradually increases to a peak, then declines as the motor accelerates toward stable operation. As reported in Table 2, Test 6 recorded a maximum power of 200 W at 0.6 seconds after activation. Power subsequently decreased to 184 W at 0.8 seconds and 165 W at 1.0 seconds, indicating reduced demand following the initial startup phase. After the transient period, power stabilized at approximately 90–91 W within 3.5 seconds. The large difference between peak and steady-state power shows that startup requires much more power than normal operation. Therefore, system performance evaluation should consider not only steady-state consumption but also peak power and transient duration to determine energy-source capacity adequacy and the operational reliability of photovoltaic-based pumping systems.

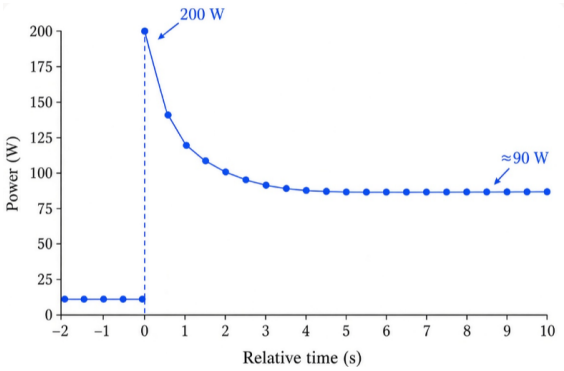


Figure 3. Transient Power Profile during a Single Starting Process of an AC Pump

Figure 3 illustrates three primary phases of the system's power characteristics: the pre-startup condition, the transient startup phase, and the steady-state condition. Before the pump is started, the recorded power is 13 W. After the start command,

power rises to a peak of 200 W before gradually decreasing and stabilizing at approximately 90–91 W. This increase represents the total power response of all loads measured at the measurement point during pump start-up. However, to determine the pump's power consumption more accurately, it is necessary to verify whether the 13 W baseline power originates from auxiliary devices or other components connected to the same measurement point. If this power represents auxiliary equipment consumption, it must be accounted for in the analysis to separate the pump's power contribution from the system's baseline consumption. This distinction enables a more precise interpretation of the power curve, particularly when comparing the power requirements during startup with those under steady-state operating conditions.

Table 3. Real-time Power and Transient Parameters during the Starting Process

Test	Time	P0 (W)	Ppeak (W)	Pss (W)	Kp	tpeak (s)	ttr (s)	Description
1	11:30	13	125	89	1.40	0.8	2.8	Starting normally
2	11:40	13	138	90	1.53	0.7	3.0	Starting normally
3	11:50	13	152	91	1.67	0.9	3.1	Surge increasing
4	12:00	13	166	90	1.84	0.8	3.3	Quite high transient
5	12:10	13	181	92	1.97	0.7	3.5	High surge
6	12:20	13	200	91	2.20	0.6	3.8	Highest peak
7	12:30	13	174	90	1.93	0.8	3.4	High surge
8	12:40	13	158	89	1.78	0.9	3.2	Beginning to decrease
9	12:50	13	144	90	1.60	1.0	3.0	Starting normally
10	13:00	13	132	88	1.50	1.1	2.9	Relatively low surge

Table 3 presents results from ten pump-startup tests, including P0, Ppeak, Pss, Kp, tpeak, and ttr. Ppeak ranged from 125 to 200 W, with a mean of 157.0 W and a standard deviation of 23.57 W. In contrast, Pss ranged from 88 to 92 W, with a mean of 90.0 W and a standard deviation of 1.15 W. The coefficient of variation was approximately 15.0% for Ppeak and 1.28% for Pss, indicating greater variability during startup than during steady-state operation. This difference may reflect factors such as the power source, hydraulic load, battery voltage, inverter response, and measurement methodology.

The Kp values ranged from 1.40 to 2.20, with a mean of 1.74 ± 0.25. The highest value occurred in Test 6, where the peak power of 200 W was approximately 2.20 times the steady-state power of 91 W. On average, the peak startup power of 157 W was approximately 74.44% higher than the mean steady-state power of 90 W. These findings indicate that inverter selection should not be based solely on steady-state power requirements. Furthermore, tpeak ranged from 0.6 to 1.1 s, with a mean of 0.83 ± 0.15 s, while ttr ranged from 2.8 to 3.8 s, with a mean of 3.20 ± 0.31 s. Transient duration matters because an inverter's ability to start a motor depends on both the magnitude of the power demand and how long the demand persists. Therefore, inverters with identical continuous power ratings may differ in their motor-starting capabilities depending on their surge-power specifications and protection strategies.

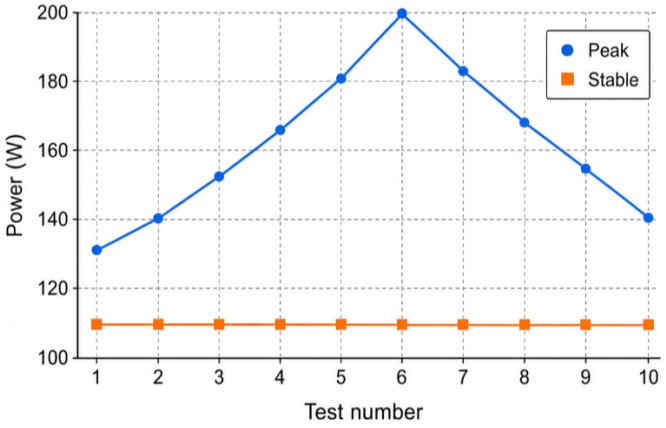


Figure 4. Comparison of Peak Power and Steady-State Power Across 10 Tests

Figure 4 illustrates the variation in peak and steady-state power across the ten pump-startup tests. Peak power increased from 131 W in Test 1 to a maximum of 200 W in Test 6, then gradually decreased to 140 W in Test 10. In contrast, the steady-state power remained relatively constant at approximately 109 W throughout the tests. This pattern indicates that the largest power variations occurred during startup, whereas steady-state power showed minimal variation. The difference between the peak and steady-state power highlights the additional power demand associated with starting the pump. However, these values represent the power recorded by the measuring instrument and should not be interpreted as instantaneous electrical peaks.

5. Discussion

The findings demonstrate that AC pump startup is associated with greater power demand and variability than steady-state operation. Across the ten tests, peak startup power ranged from 125 to 200 W, while steady-state power ranged from 88 to 92 W. The mean peak power of 157.0 W was 74.44% higher than the mean steady-state power of 90.0 W. This difference reflects the additional electrical demand during motor startup and acceleration. The relatively low variation in steady-state power, compared with peak startup power, indicates that the most substantial power fluctuations occurred during the transition to normal operation. This pattern is consistent with Habyarimana et al. (2022) and Mahadewi et al. (2026) on induction motor starting, which identify starting current and potential voltage sags as important characteristics of motor operation. In photovoltaic water pumping systems, these characteristics are relevant because the electrical supply must accommodate both the initial startup demand and the subsequent operating load (Arisman & Iwan, 2023; Arisman et al., 2026).

The Kp ranged from 1.40 to 2.20, with a mean of 1.74. The highest ratio occurred in Test 6, when the recorded peak power reached 200 W against a steady-state power of 91 W. This finding illustrates the difference between the power required during startup and that required during normal operation. However, the observed active power ratio should not be equated directly with the starting-current ratios commonly reported for induction motors because current and active power represent different electrical quantities. Moreover, the values in this study were obtained from a power-measuring instrument's display, which may not capture rapid electrical fluctuations during the initial AC cycles. Research by Suwito et al. (2022) and Setyowati et al. (2026) on motor starting has examined the relationship between starting current and voltage disturbances, while studies of photovoltaic pumping systems have addressed the role of power converters and motor-drive configurations

in system operation. The present findings complement these studies by quantifying the startup-to-steady-state active power relationship in the tested off-grid PV pumping prototype.

The temporal characteristics further show that the startup process extends beyond the recorded peak. The time to peak power ranged from 0.6 to 1.1 s, with a mean of 0.83 s, whereas the transient duration ranged from 2.8 to 3.8 s, with a mean of 3.20 s. This difference indicates that the maximum recorded power occurs relatively early in the startup process, followed by a period in which power decreases toward its steady-state level. This behavior is relevant to understanding motor-starting dynamics because the startup event involves both a temporary power increase and a subsequent transition to stable operation. Previous research by Rengma et al. (2023), Pardo and Navarro-Gonzalez (2024), and Saady et al. (2025) on photovoltaic water pumping systems has emphasized MPPT optimization, motor control, and system configuration. Research on PV-powered motor-driven pumping systems has also examined converter and drive configurations (Prabhakaran et al., 2022; Arumas et al., 2026). Compared with these approaches, the present study focuses specifically on the measurable power profile during the startup of an AC pump, describing its peak magnitude and temporal characteristics rather than optimizing the control system.

The results also show the value of examining startup and steady-state power together when characterizing an off-grid PV pumping system. The relatively stable steady-state values contrast with the wider variation in peak startup power across the ten tests, showing that the two operating phases vary differently. This distinction complements broader reviews of solar and hybrid water pumping systems, which discuss the electrical configurations and operating characteristics involved in supplying pumping loads (Mahmood & Hashjin, 2022). Research by Kumar et al. (2022) and Bawa et al. (2025) on photovoltaic pumping applications has also considered system sizing, energy management, and performance under different operating configurations. By focusing on power measurements recorded during startup, this study adds an empirical characterization of transient load behavior to the analysis of a small-scale off-grid PV pumping prototype. The findings distinguish the recorded peak power from steady-state consumption and describe how the observed power profile changes over time during pump startup.

6. Conclusion

This study characterized the startup power profile of an AC pump in an off-grid solar photovoltaic system using video recordings of a power-measuring instrument. Across ten tests, peak startup power ranged from 125 to 200 W, averaging 157.0 W, while steady-state power ranged from 88 to 92 W, averaging 90.0 W. Mean peak power was approximately 74.44% higher than mean steady-state power. The Kp ranged from 1.40 to 2.20, with a mean of 1.74. Time to peak ranged from 0.6 to 1.1 s, and transient duration ranged from 2.8 to 3.8 s. These results indicate distinct power characteristics during startup and steady-state operation, with greater variability in peak startup power.

Steady-state power alone may underestimate startup demand in off-grid PV pumping systems. Inverter selection should therefore consider startup power and transient duration alongside continuous power requirements. However, the observed peak represents the highest value the instrument captured, not necessarily the instantaneous electrical peak. The 13 W pre-startup baseline also requires verification to determine whether it originates from auxiliary loads or other components at the measurement point. This study is limited by display-based video recording, which may not capture rapid sub-cycle fluctuations, and by testing a single prototype. Future research should measure voltage and current simultaneously using a power analyzer or high-speed data logger, assess power

factor, apparent power, and voltage sag, and repeat tests under different pump loads, battery conditions, irradiance levels, and inverter configurations.

References

Angadi, S., Yaragatti, U. R., Suresh, Y., & Raju, A. B. (2021). Comprehensive review on solar, wind and hybrid wind-PV water pumping systems-an electrical engineering perspective. *CPSS Transactions on Power Electronics and Applications*, *6*(1), 1-19. https://doi.org/10.24295/CPSSTPEA.2021.00001.

Arisman, A., & Iwan, I. (2023). Effectiveness of solar panel-based street lights and their impact on environmental sustainability. *Research Horizon*, *3*(6), 646–654. https://doi.org/10.54518/rh.3.6.2023.189.

Arisman, A., Alatas, M., Kurniawan, A., & Ridlo, D. T. (2026). Microgrid-based energy-independent village planning through identification of rooftop solar power plants potential in Kedungrong, Yogyakarta. *International Journal of Environmental Impacts*, *9*(5), 973–985. https://doi.org/10.56578/ijei090503

Arumas, A. R., Widyartono, M., Wardani, A. L., & Rahmadian, R. (2026). Pengembangan sistem pompa air otomatis berbasis PLTS off-grid untuk irigasi sawah. *Elposys: Jurnal Sistem Kelistrikan*, *13*(2), 46–51. https://doi.org/10.33795/elposys.v13i2.9487.

Bahramian, M. A., Ebadi, M., Ghadimi, A. A., & Khalili, M. (2025). Starting electro-motor loads in battery-less off-grid photovoltaics using a super-capacitor based charge-pump. *Journal of Power Sources*, *626*(1), 235-245. https://doi.org/10.1016/j.jpowsour.2024.235694.

Bawa, A.-R., Amponsah, W., & Quansah, D. A. (2025). Design, simulation, and economic analysis of a solar photovoltaic-powered pumping system for drip irrigation of a 1-ha bean farm in a tropical climate. *Journal of Engineering*, *2025*(1), 166-172. https://doi.org/10.1155/je/1662260.

Belgacem, F., Mostefai, M., Yahia, M., & Belgacem, A. (2022). Optimization of photovoltaic water pumping system based on BLDC motor for agricultural irrigation with different MPPT methods. *Periodica Polytechnica Electrical Engineering and Computer Science*, *66*(4), 315–324. https://doi.org/10.3311/PPee.20140.

Benlarbi, K., Mokrani, L., & Nait-Said, M. S. (2004). A fuzzy global efficiency optimization of a photovoltaic water pumping system. *Solar Energy*, *77*(2), 203-216. https://doi.org/10.1016/j.solener.2004.03.025.

Caracas, J. V. M., de Carvalho Farias, G., Teixeira, L. F. M., & de Souza Ribeiro, L. A. (2013). Implementation of a high-efficiency, high-lifetime, and low-cost converter for an autonomous photovoltaic water pumping system. *IEEE Transactions on Industry Applications*, *50*(1), 631-641. https://doi.org/10.1109/TIA.2013.2271214.

Gevorkov, L., Domínguez-García, J. L., & Romero, L. T. (2022). Review on solar photovoltaic-powered pumping systems. *Energies*, *16*(1), 1-12. https://doi.org/10.3390/en16010094.

Habyarimana, M., Dorrell, D. G., & Musumpuka, R. (2022). Reduction of starting current in large induction motors. *Energies*, *15*(10), 3848-3858. https://doi.org/10.3390/en15103848.

Hermawan, I. B., Mochamad, A., & Riawan, D. C. (2023). Designing a smart inverter for voltage sag compensation due to motor start-up. *Kinetik: Game Technology, Information System, Computer Network, Computing, Electronics, and Control*, *8*(3), 663–672. https://doi.org/10.22219/kinetik.v8i3.1744.

Ismail, F. B., Rahmat, M. A. A., Kazem, H. A., Al-Obaidi, A. S. M., & Ridwan, M. S. (2024). Maximizing energy via solar-powered smart irrigation: An approach utilizing a single-axis solar tracking mechanism. *Irrigation and Drainage*, *73*(3), 829–845. https://doi.org/10.1002/ird.2937.

Kolhe, M., Joshi, J. C., & Kothari, D. P. (2004). Performance analysis of a directly coupled photovoltaic water-pumping system. *IEEE Transactions on Energy Conversion*, *19*(3), 613-618. https://doi.org/10.1109/TEC.2004.827032.

Kumar, L. A., Lakshmiprasad, C. N., Ramaraj, G., & Sivasurya, G. (2022). Design, simulation of different configurations and life-cycle cost analysis of solar photovoltaic–water-pumping system for agriculture applications: Use cases and implementation issues. *Clean Energy*, *6*(2), 335–352. https://doi.org/10.1093/ce/zkac018.

Mahadewi, N. K. N., Gunamantha, I. M., & Sudiana, I. K. (2026). Estimation of methane emissions using the IPCC FOD model with local parameters and mitigation analysis. *Research Horizon*, *6*(3), 1491–1508. https://doi.org/10.54518/rh.6.3.2026.1168.

Mahmood, F. M., & Hashjin, M. R. (2022). Starting analysis of squirrel cage induction motors 1000 kW by variable frequency drive in power system, case study: Tabriz pump station. *NTU Journal of Engineering and Technology*, *1*(4), 400-412. https://doi.org/10.56286/ntujet.v1i4.369

Pardo, M. A., & Navarro-Gonzalez, F. J. (2024). Sizing and scheduling optimisation method for off-grid battery photovoltaic irrigation networks. *Renewable Energy*, *221*(11), 1198-1212. https://doi.org/10.1016/j.renene.2023.119822.

Periasamy, P., Jain, N. K., & Singh, I. P. (2015). A review on development of photovoltaic water pumping system. *Renewable and Sustainable Energy Reviews*, *43*(9), 918-925. https://doi.org/10.1016/j.rser.2014.11.019.

Prabhakaran, K. K., Sunkara, V., & Karthikeyan, A. (2022). Single-stage PV-powered boost inverter-fed permanent-magnet synchronous motor-driven water-pumping system. *Clean Energy*, *6*(5), 726–737. https://doi.org/10.1093/ce/zkac053.

Rengma, N. S., Yadav, M., & Kishor, N. (2023). Solar photovoltaic water pumping system: A software tool development-based optimal configuration investigation for system installation location, sizing and deployment. *Renewable Energy Focus*, *46*(2), 236–255. https://doi.org/10.1016/j.ref.2023.07.001.

Saady, I., Majout, B., Bossoufi, B., Karim, M., Elkafazi, I., Merzouk, S., Almalki, M. M., Alghamdi, T. A. H., Skruch, P., Zhilenkov, A., & Mobayen, S. (2025). Improving photovoltaic water pumping system performance with PSO-based MPPT and PSO-based direct torque control using real-time simulation. *Scientific Reports*, *15*(1), 16-27. https://doi.org/10.1038/s41598-025-00297-8.

Setyowati, E., Yuan, A., & Dharmawanti, S. (2026). Performance assessment of a solar water pumping system under high-head conditions in Sumba, Indonesia. *Lontar Physics Today*, *5*(1), 157–171. https://doi.org/10.26877/lpt.v5i1.354.

Singh, B., & Shukla, S. (2018). Induction motor drive for PV water pumping with reduced sensors. *IET Power Electronics*, *11*(12), 1903–1913. https://doi.org/10.1049/iet-pel.2017.0856.

Singh, B., Sharma, U., & Kumar, S. (2018). Standalone photovoltaic water pumping system using induction motor drive with reduced sensors. *IEEE Transactions on Industry Applications*, *54*(4), 3645-3655. https://doi.org/10.1109/TIA.2018.2825285.

Suratno, S., & Cahyono, B. D. (2023). Rancang bangun sistem pembangkit listrik tenaga surya (PLTS) sebagai catu daya pompa air submersible. *Jurnal Teknik Elektro Uniba (JTE UNIBA)*, *7*(2), 309–319.

Suwito, S., Ashari, M., Rivai, M., & Mustaghfirin, M. A. (2022). Enhancement of photovoltaic pressurized irrigation system based on hybrid Kalman fuzzy. *International Journal of Intelligent Engineering and Systems*, *15*(2), 426–440. https://doi.org/10.22266/ijies2022.0430.39.

Wanyama, J., Soddo, P., Nakawuka, P., Tumutegyereize, P., Bwambale, E., Oluk, I., Mutumba, W., & Komakech, A. J. (2023). Development of a solar powered smart irrigation control system kit. *Smart Agricultural Technology*, *5*(1), 100-112. https://doi.org/10.1016/j.atech.2023.100273

Yogaswara, K. B. A., & Korry, P. D. P. (2025). Application of the house of risk for operational risk mitigation in regional public water utilities. *Research Horizon*, *5*(6), 2547–2564. https://doi.org/10.54518/rh.5.6.2025.903

Zhou, K., Ma, X., Gao, F., Yao, J., & Kan, X. (2024). Frequency optimisation and performance analysis of photovoltaic-battery water pumping system. *Renewable Energy*, *230*(1), 120-128. https://doi.org/10.1016/j.renene.2024.120844.

Acknowledgment
The authors express gratitude to the Institut Teknologi Yogyakarta and DRTPM for their support regarding facilities and the execution of the research.

Funding Information
This research did not receive any funding.

Conflict of Interest Statement
The authors declare that there is no conflict of interest.

Ethical Approval and Originality Statement
Ethical approval was obtained for this study. The manuscript represents original work and has not been previously published, nor is it under consideration by another journal.

Data Disclosure Statement
The data that support the findings of this study are available from the corresponding author upon reasonable request.



Copyright: © 2026 by the authors.
This work is licensed under the terms and conditions of the Creative Commons Attribution-ShareAlike 4.0 International License (https://creativecommons.org/licenses/by-sa/4.0/).